MICROBIOLOGY

RESEARCH ARTICLE

Li *et al.*, *Microbiology* 2023;169:001337

DOI 10.1099/mic.0.001337

MICROBIOLOGY SOCIETY

OPEN ACCESS

PF-431396 hydrate inhibition of kinase phosphorylation during adherent-invasive *Escherichia coli* infection inhibits intra-macrophage replication and inflammatory cytokine release

Xiang Li[1], Michael J. Ormsby[1]†, Ghaith Fallata[1,2], Lynsey M. Meikle[1], Daniel Walker[3], Damo Xu[1,4] and Daniel M. Wall[1,*]

Abstract

Adherent-invasive *Escherichia coli* (AIEC) have been implicated in the aetiology of Crohn's disease (CD). They are characterized by an ability to adhere to and invade intestinal epithelial cells, and to replicate intracellularly in macrophages resulting in inflammation. Proline-rich tyrosine kinase 2 (PYK2) has previously been identified as a risk locus for inflammatory bowel disease and a regulator of intestinal inflammation. It is overexpressed in patients with colorectal cancer, a major long-term complication of CD. Here we show that Pyk2 levels are significantly increased during AIEC infection of murine macrophages while the inhibitor PF-431396 hydrate, which blocks Pyk2 activation, significantly decreased intramacrophage AIEC numbers. Imaging flow cytometry indicated that Pyk2 inhibition blocked intramacrophage replication of AIEC with no change in the overall number of infected cells, but a significant reduction in bacterial burden per cell. This reduction in intracellular bacteria resulted in a 20-fold decrease in tumour necrosis factor α secretion by cells post-AIEC infection. These data demonstrate a key role for Pyk2 in modulating AIEC intracellular replication and associated inflammation and may provide a new avenue for future therapeutic intervention in CD.

INTRODUCTION

Crohn's disease (CD) is characterized by chronic inflammation of the gastrointestinal tract, most commonly affecting the terminal ileum and proximal colon. A histopathological hallmark of CD is the aggregation of intestinal macrophages, resulting in lesions, referred to as granulomas [1, 2]. The initial trigger of CD remains unknown, but the aetiology of CD involves environmental factors, infectious agents and genetic predisposition. Together these lead to an abnormal mucosal immune response to pathogenic insult and alterations in both microbial composition and metabolic activity of intestinal communities [3]. Dysbiosis in CD patients is observed as an overall reduction in gut microbial diversity and an overgrowth of pro-inflammatory bacteria including *Enterobacteriaceae*. In particular, a pathovar of *Escherichia coli* known as adherent-invasive *E. coli* (AIEC) increases in prevalence during inflammation and has been detected in the ileal mucosa of CD patients at higher levels compared to healthy controls (21.7%–36.4% versus 6.2%) [4–6]. Other studies have directly implicated AIEC in the aetiology of CD [6, 7].

Once AIEC cross the intestinal epithelium, they are phagocytised by macrophages into a degradative organelle, termed a phagolysosome [8], that is equipped with a broad range of lytic enzymes [9, 10]. AIEC have acquired several factors that are essential for evading phagolysosome degradation; including tolerance of acidic pH and nutritional and oxidative stress [11]. However,

Received 13 January 2023; Accepted 02 May 2023; Published 13 June 2023

Author affiliations: [1]School of Infection and Immunity, College of Medical, Veterinary and Life Sciences, Sir Graeme Davies Building, University of Glasgow, Glasgow G12 8TA, UK; [2]Department of Basic Science, College of Science and Health Professions, King Saud bin Abdulaziz University for Health Sciences, Jeddah 22384, Saudi Arabia; [3]Strathclyde Institute for Pharmacy and Biomedical Sciences, University of Strathclyde, Glasgow G4 0RE, UK; [4]State Key Laboratory of Respiratory Disease for Allergy at Shenzhen University, Shenzhen Key Laboratory of Allergy & Immunology, Shenzhen University School of Medicine, Shenzhen, PR China.

***Correspondence:** Daniel M. Wall, donal.wall@glasgow.ac.uk

Keywords: AIEC; intracellular replication; Pyk2; TNFα.

Abbreviations: AIEC, adherent-invasive *E. coli*; CD, crohn's disease; c.f.u., colony forming units; FAK, focal adhesion kinase; FBS, foetal bovine serum; f.f.u., fluorescence focus units; h p.i., hours post-infection; IBD, inflammatory bowel disease; IFC, imaging flow cytometry; LDH, lactate dehydrogenase; PAMPs, pathogen associated molecular patterns; PRRs, pattern recognition receptors; PYK2, proline-rich tyrosine kinase; TNFα, tumour necrosis factor α.

†Present address: Biological and Environmental Sciences, Faculty of Natural Science, University of Stirling, Stirling, FK49 4LA, UK.

Four supplementary figures are available with the online version of this article.

the ability of AIEC to survive within the harsh environment of a macrophage with the concomitant release of tumour necrosis factor α (TNFα) is still poorly understood.

Intestinal macrophages enriched in the lamina propria, capture and eliminate any bacteria that cross the epithelial barrier and are responsible for clearing apoptotic and senescent epithelial cells [12]. These sub-epithelial macrophages are essential for maintenance of mucosal homeostasis in the presence of the microbiota and also play a pivotal role in protective immunity against pathogens [13]. Macrophages mount their response against microbial pathogens through binding of pattern recognition receptors (PRRs) to pathogen-associated molecular patterns (PAMPs) resulting in release of a variety of proinflammatory cytokines and chemoattractants, such as TNFα. This cytokine is a key mediator of inflammation in CD, disrupting epithelial barrier function by altering the structure and function of tight junctions [14, 15]. A milestone in treating CD was the introduction of anti-TNFα agents, like infliximab and adalimumab [16, 17].

Large-scale genome-wide association studies in cohorts of European patients resulted in the identification of candidate genes in inflammatory bowel disease (IBD) susceptibility loci [18]. These included proline-rich tyrosine kinase 2 (*PYK2*), a non-receptor, Ca^{2+} dependent protein-tyrosine kinase that is expressed in numerous tissues and cell types and which is involved in innate immunity [19]. More recently PYK2 has been implicated in the regulation of the inflammatory response in the human gut and has been suggested as a therapeutic intervention target in IBD [20]. It is highly expressed in the central nervous system, epithelial cells, hematopoietic cells, and it is also over-expressed in various cancers [21, 22]. Activation of PYK2 involves autophosphorylation at Tyr-402, which enables the binding of Src via the SH2 domain and phosphorylation of PYK2 at Tyr-579 and Tyr-580, within the kinase domain activation loop, to generate maximal kinase activity [23]. Phosphorylated PYK2 functions in the regulation of phagocytosis, migration, proliferation, invasion, oncogenesis and metastasis, and has been directly implicated in the control of intestinal inflammation [22, 24–26]. In macrophages, Pyk2 has defined functions in regulating morphology, migration and phagocytosis [22, 27, 28]. Absence of Pyk2, and focal adhesion kinase (FAK), leads to spontaneous colitis in mice with the role of these kinases in intestinal epithelial repair thought to underlie this phenotype [29]. Additionally Pyk2 regulates neutrophil adhesion and activation, directly controlling reactive oxygen species (ROS) generation [30]. Given the diversity of Pyk2 function it is therefore considered a valuable therapeutic target in various disease states, such as inflammation and cancer [31].

In this study, the role of Pyk2 in facilitating intracellular replication of the AIEC type-strain LF82 in murine macrophage cells was determined. Through the use of high-throughput imaging of individual cells via imaging flow cytometry, we have gained an increased understanding of the role of this kinase at the single-cell level, demonstrating a key role for the Pyk2/FAK axis in controlling intramacrophage replication of this poorly understood pathogen.

METHODS

Bacterial strains and culture conditions

The adherent-invasive *E. coli* (AIEC) type strain LF82 used in this study was cultured in lysogeny-broth (LB) at 37 °C with shaking at 180 r.p.m. [32]. Prior to infection, LF82 was grown overnight in Roswell Park Memorial Institute (RPMI)-1640 media (Life Technologies) supplemented with 3% heat-inactivated foetal bovine serum (FBS) (Sigma), and 1% L-glutamine. *In vitro* infections were carried out using LF82 transformed with a reporter plasmid, pAJR70 expressing eGFP under the control of the *rpsM* promoter [33]. GFP expression was measured in a black 96-well plate (excitation at 485 nm; emission at 550 nm) using a FLUOstar Optima Fluorescence Plate Reader (BMG Labtech).

Maintenance of RAW 264.7 cells

The RAW 264.7 murine macrophage-like cell line was obtained from the American Type Culture Collection (ATCC). RAW 264.7 cells were cultured in RPMI-1640 media supplemented with 10% heat-inactivated FBS, 1% penicillin/streptomycin, and 1% L-glutamine (maintenance media) at 37 °C in 5% CO_2.

Gentamicin protection assay for AIEC infection

RAW 264.7 cells were seeded onto a 24-well plate at a density of 2×10^5 cells-per-well 24 h prior to infection (h p.i.). Twelve hours prior to infection, maintenance media was replaced with RPMI-1640 media supplemented with 3% FBS and 1% L-glutamine containing lipopolysaccharide (LPS 1 μg ml^{-1}) for activation. Cells were infected at a m.o.i. of 100 and incubated at 37 °C/5% CO_2 for 1 h. After 1 h the infected RAW 264.7 cells were washed twice with fresh RPMI cell-culture media to remove excess extracellular bacteria and incubated at 37 °C/5% CO_2 in maintenance media with 50 μg ml^{-1} gentamicin to kill any remaining extracellular bacteria. In addition to gentamicin, cell-culture media was also supplemented where indicated with the Pyk2 and FAK inhibitor PF-431396-hydrate [34]. The infected cells were then incubated for the time specified at 37 °C/5% CO_2.

To measure AIEC intra-macrophage survival, infected macrophages were washed with RPMI-1640 media and lysed using 200 μl of 2% Triton X-100 in PBS for 5 min at room temperature. Lysates were removed, serially diluted in PBS, and plated onto LB agar plates to determine the number of c.f.u. per ml. Total protein concentration was determined using a BCA assay (Thermofisher)

and bacterial numbers were normalized to total protein concentration and presented as c.f.u./g. Normalizing c.f.u. to protein concentration, as opposed to expressing c.f.u. numbers per well, meant c.f.u. could be related to cell number in each individual well, especially important if cell numbers differed between wells due to proliferation or cell death during infection or drug treatment.

AIEC phagocytosis assay

RAW 264.7 cells were plated in a 24-well plate at a density of 2×10^5 cells-per-well. Cells were incubated (37 °C, 5% CO_2) for 6 h resulting in adherence to plates. Before infection, cells were activated by adding 1 μg ml^{-1} of LPS 12 h prior to infection. Activated cells were treated with the indicated concentrations of PF-431396 hydrate (Sigma-Aldrich) for 1 h. PF-431396 hydrate inhibits activity of both Pyk2 and FAK, suppressing the phosphorylation of Pyk2 at its active tyrosine phosphorylation site (Y402) without decreasing total protein level of Pyk2, thus functionally blocking multiple cellular signalling pathways [35]. Supernatants were removed and cells were infected with a m.o.i. of 100 in 200 μl of RPMI-1640 media containing 3% FBS and 1% L-glutamine. Cells were left for 1 h to allow bacterial phagocytosis to occur, before the supernatant was removed and 1 ml of fresh media containing gentamicin (50 μg ml^{-1}) was added for 1 h to kill any extracellular bacteria. Post-gentamicin treatment, supernatants were removed, cells were lysed with 200 μl PBS containing 2% Triton X-100 for 5 min and bacteria numbers calculated as described above.

Lactate dehydrogenase assay to monitor cytotoxicity

RAW 264.7 cells were infected at a m.o.i. of 100 and supernatants of LF82 infected and control macrophages were sampled at different time points of gentamicin treatment, centrifuged at 10000 ***g*** for 4 min and assayed for lactate dehydrogenase (LDH) activity (Sigma). LDH activity is reported as milliunit/ml. One unit of LDH activity is defined as the amount of enzyme that catalyses the conversion of lactate into pyruvate to generate 1 μmol of NADH per minute at 37 °C.

Western blotting

LF82 infected and control cells were lysed at 6 h post-infection (h p.i.) for 15 min in radioimmunoprecipitation assay (RIPA) lysis buffer (ThermoFisher) supplemented with protease inhibitor (Sigma) and phosphatase inhibitor (Sigma). Lysates were centrifuged at 14000 ***g*** for 10 min. The protein concentration of the cell extracts was determined using the BCA assay kit (Bio-Rad). Protein concentration for lysates was adjusted to 2 μg μl^{-1} before adding 4X loading buffer (ThermoFisher), heating to 95 °C for 10 min and running on an SDS-PAGE gel. Samples were transferred via electrophoretic wet transfer to a polyvinylidene fluoride (PVDF) membrane. The membrane was blocked in 5% non-fat milk and probed with a 1:1000 dilution of anti-Pyk2 (Abcam) or a 1:1000 dilution of anti-phosphorylated Pyk2 (ab4800; Abcam). Blots were visualized with HRP-conjugated goat anti-rabbit antibody (1:10,000) or HRP-conjugated goat anti-mouse (1:10,000) (ThermoFisher) and developed using enhanced chemiluminescence (ECL) and imaged using a C-DiGit blot scanner (LI-COR). Membranes were stripped in 0.1 mM glycine, pH 2.2, and re-probed with anti-GAPDH (1:10,000; Abcam) antibody as a loading control. The bands were quantified using ImageJ software [36]. To compare both Pyk2 and pPyk2 levels in infected or uninfected RAW 264.7 cells with or without PF-431396 hydrate treatment, values from each blot were normalized by loading control (GAPDH) as Pyk2/GAPDH or pPyk2/GAPDH. The Pyk2/GAPDH and pPyk2/GAPDH values of control groups were set as one and the relatively densitometric change of test samples was calculated. All Western blots were performed in triplicate, with each performed on a biological replicate. All data are represented as the mean ± standard deviation for all performed repetitions.

Imaging flow cytometry

Imaging-flow-cytometry (IFC) data acquisition was achieved using an ImageStream X MKII (Amnis) equipped with dual cameras and 405, 488 and 642 nm excitation lasers. All samples were acquired at 60 times magnification giving an optimal 7 μM visual slide through the cell, and a minimum of 10000 single cell events were collected for each sample. In focus cells were determined by a gradient root mean square (RMS) for image sharpness. Brightfield of greater than 50 and single cells were identified by area versus aspect ratio. Only data from relevant channels were collected including Channel 02 (Ch02, GFP fluorescence), Ch04 (bright field) and Ch05 (pPyk2 conjugated AF647 fluorescence). Samples were run with a 488 nm laser with power of 5 mW and a 642 nm laser with power of 150 mW. Single colour compensation controls were also acquired, and a compensation file generated via IDEAS software (Luminex).

Imaging-flow-cytometry data analysis

Data analysis for samples collected using the ImageStream X MKII was performed using IDEAS. Masks (area of interest) and features (calculations made from masks) were generated to give quantitative measurements of the images collected. To quantify intracellular bacteria, a mask was created to select just the intracellular portion of the cell, in this case referred to as an AdaptiveErode mask. To analyse fluorescent spots (representative of bacterial burden per cell), a spot count mask was created in the reference channel for GFP bacteria (Ch02).

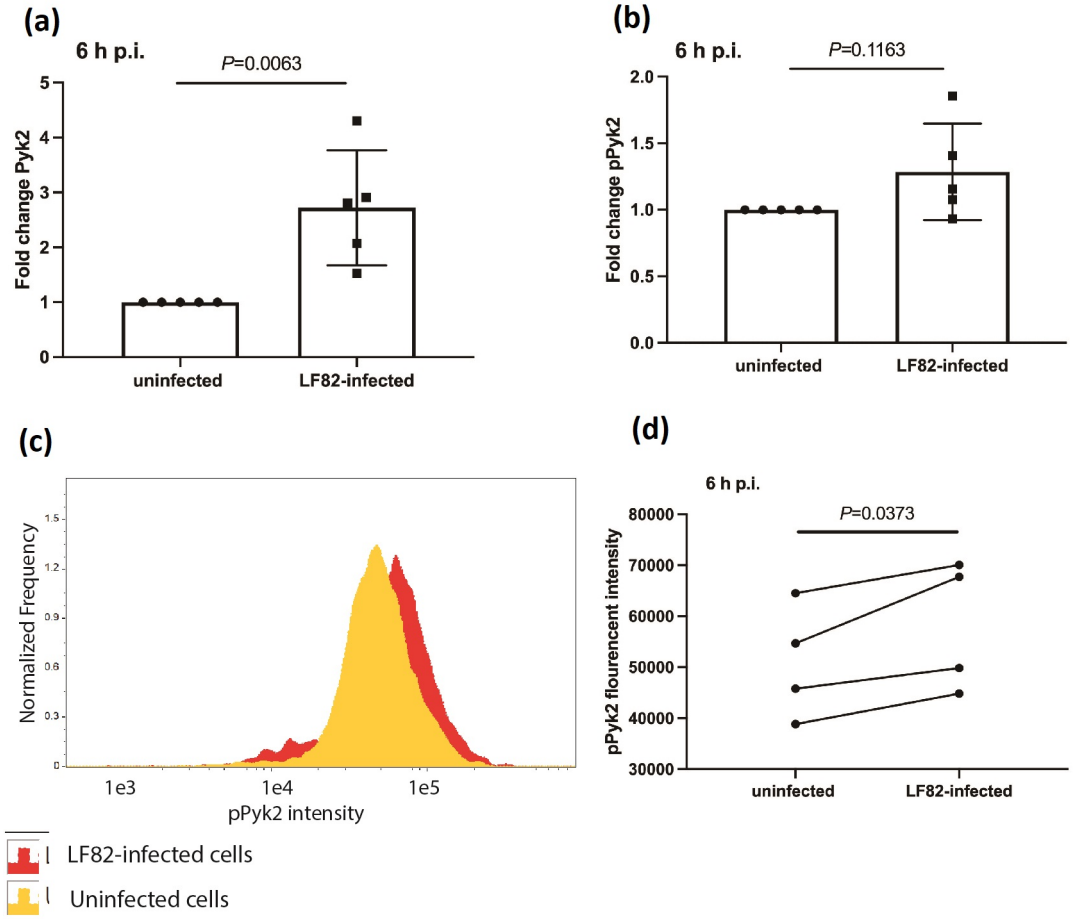

Fig. 1. Pyk2 and phosphorylated Pyk2 (pPyk2 [Y402]) expression levels in RAW 264.7 macrophages. (a) Levels of Pyk2 or (b) pPyk2 (Y402) at 6 h p.i. were compared between LF82-infected or uninfected RAW 264.7 cells using densitometric analysis of Western blots. Bands from infected cells were analysed by densitometry and compared to control uninfected cells using ImageJ and fold change in (a) Pyk2 and (b) pPyk2 (Y402) levels are shown. Statistical analyses were conducted using Student's *t*-test. (c) A representative histogram showing imaging flow cytometry data displays the pPyk2 (Y402) intensity of control uninfected RAW 264.7 macrophages in yellow and LF82 infected cells at 6hpi in red. (d) The level of pPyk2 (Y402) in infected RAW 264.7 cells at 6 h p.i. was analysed by imaging flow cytometry and compared with that of uninfected cells, using a paired *t*-test statistical analysis. Results are representative of at least four independent experiments.

Enzyme-linked immunosorbent assays (ELISAs)

The amount of TNFα secreted in the supernatants from cell culture and cell lysate was determined by ELISA MAX Deluxe Set Mouse TNFα kit (BioLegend) according to the manufacturer's instructions. TNFα concentrations were normalized by protein concentration from cell lysates and were reported as ρg of TNFα/g of protein.

Statistical analysis

Values are shown as means and standard deviation. All statistical tests were performed with GraphPad Prism software, version 8.3.0. All replicates in this study were biological; that is, repeat experiments were performed with freshly grown bacterial cultures and cells, as appropriate. Technical replicates of individual biological replicates were also conducted. Significance was determined as indicated in the figure legends. Values were considered statistically significant when *P*-values were * = $P<0.05$; ** = $P<0.01$; *** = $P<0.001$; **** = $P<0.0001$.

RESULTS

Macrophage Pyk2 levels increase in response to LF82 infection

To determine the change in Pyk2 expression in RAW 264.7 macrophages in response to LF82 infection, total Pyk2 and phosphorylated Pyk2 (pPyk2) levels were measured by immunoblotting (Fig. 1). A significant increase in total Pyk2 was observed at 6 h

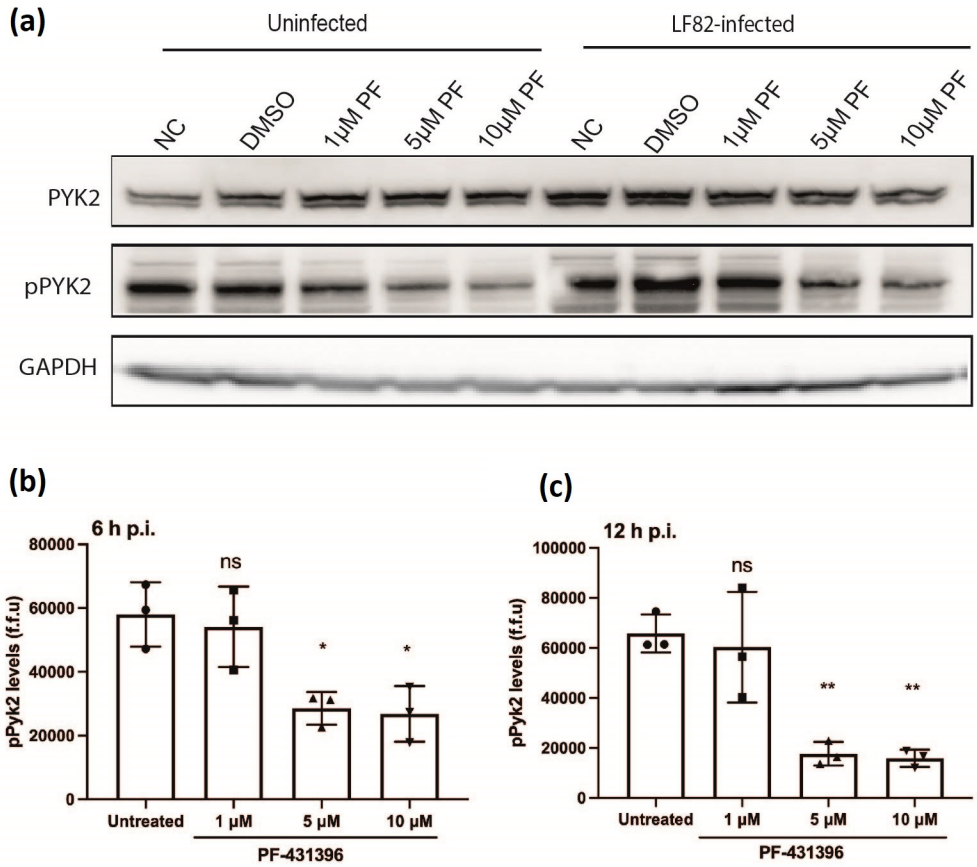

Fig. 2. The inhibitor PF-431396 hydrate blocks phosphorylation of Pyk2 in both uninfected and LF82 infected cells in a dose-dependent manner. LF82 infected or control uninfected RAW 264.7 cells were treated with PF-414396 hydrate (0, 1, 5, 10 μM) for 6 h. Untreated cells were used as controls. (a) Immunoblotting was used to detect levels of pPyk2 (Y402) with GAPDH used as loading control. To determine relative pPyk2 (Y402) levels in inhibitor treated cells, imaging-flow-cytometric analysis was conducted on LF82 infected RAW 264.7 cells after treatment for 6 h (b) or 12 h (c) with PF-431396 hydrate. Statistical analyses were conducted using a one-way ANOVA test. (ns, not significant, **P*<0.05, ***P*<0.01, ****P*<0.001). Data are representative of three independent biological replicates.

p.i. and pPyk2 levels were also increased (Fig. 1a–b). To investigate this further in relation to infection, imaging flow cytometry was used to analyse pPyk2 levels simultaneously in thousands of individual uninfected and LF82-infected cells. Imaging flow cytometry allows identification of all cells within a population that are infected with GFP-expressing bacteria. These cells can be counted and the individual bacterial load in each determined, allowing the separation of cells based on both their infection status and bacterial load in a way not possible with traditional colony counts. Using this approach here it was determined that there was a significant increase in pPyk2 levels in response to LF82 infection (Fig. 1c–d).

The inhibitor PF-431396 hydrate successfully blocks phosphorylation of Pyk2 in uninfected and LF82 infected macrophages

PF-431396 hydrate inhibits phosphorylation of Pyk2 at its active site Y402, blocking multiple cellular signalling pathways [35]. Activated Pyk2 was measured by immunoblotting cell extracts with phospho-specific antibodies directed against the Pyk2 (Y402) autophosphorylation site. Six hours post-infection levels of Pyk2 or pPyk2 (Y402) were measured by Western blot in infected cells and controls, including those where PF-431396 hydrate had been added (Fig. 2) PF-431396 hydrate significantly reduced levels of pPyk2 (Y402) in LF82-infected and uninfected RAW 264.7 cells post-treatment (5 and 10 μM; Fig. 2a).

Imaging-flow-cytometric analysis further confirmed that PF-431396 hydrate significantly reduced pPyk2 (Y402) levels in infected cells with the number of cells with detectable pPyk2 (Y402) significantly dropping at 6 h p.i. (Fig. 2b) before reducing further at 12 h p.i. (Fig. 2c). To ensure that these decreases in pPyk2 (Y402) levels were not due to cytotoxicity of PF-431396 hydrate, we demonstrated no increased release of lactate dehydrogenase (LDH) in uninfected or infected RAW 264.7 cells when PF-431396 hydrate was used at concentrations up to, and including, 10 μM (Fig. S1, available in the online version of this article).

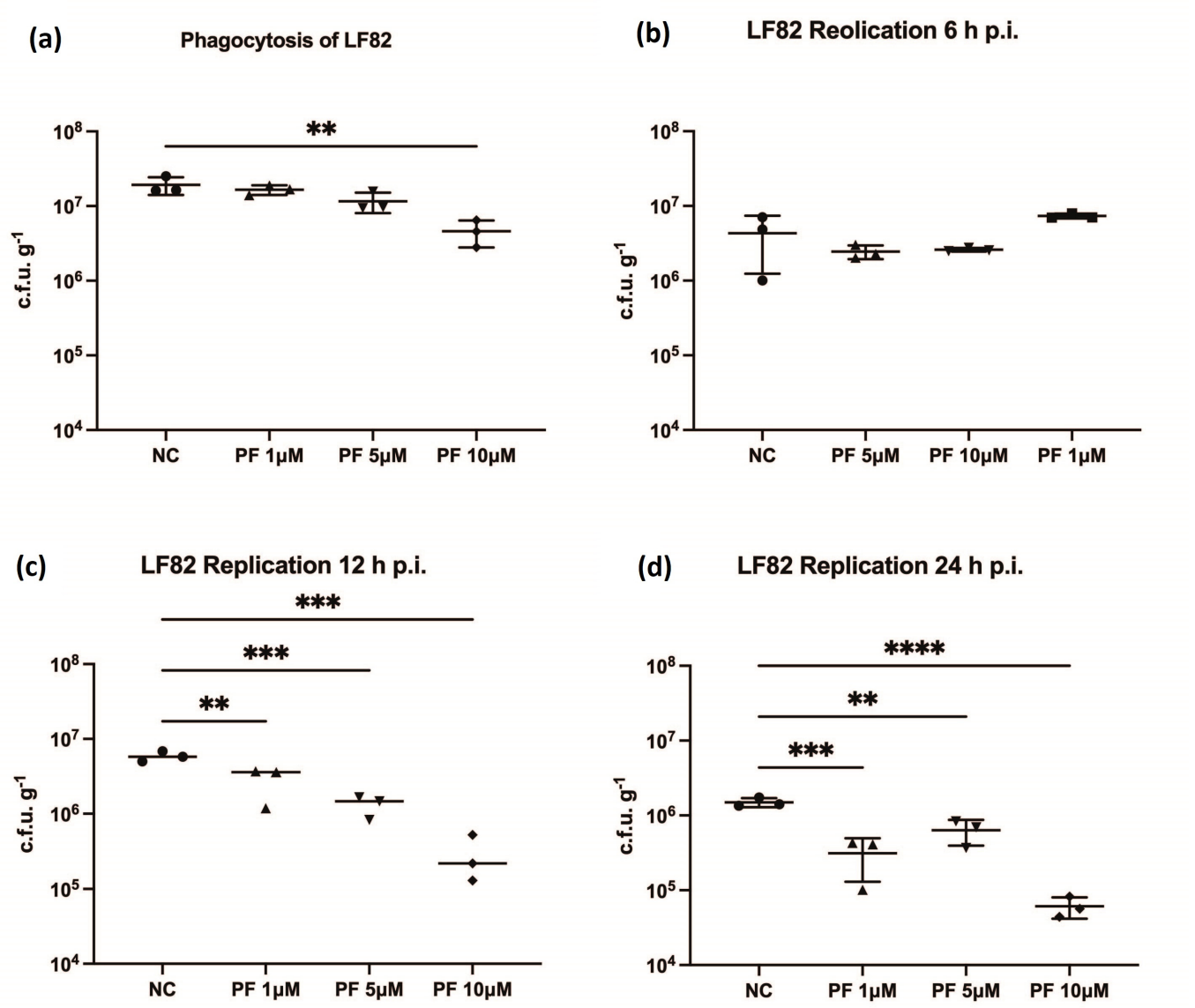

Fig. 3. Pyk2 inhibition reduces intracellular LF82 in RAW 264.7 cells. (a) (a) To determine its effect on phagocytosis of LF82, RAW 264.7 cells were pre-treated with PF-431396 hydrate for 2 h before infection with LF82 at a m.o.i. of 100. PF-431396 hydrate was added to RAW 264.7 cells at concentrations of 0 µM (NC – negative control), 1, 5 or 10 µM. DMSO in which PF-43196 hydrate was initially aliquoted was added as an additional control to ensure no residual effects of its presence on Pyk2 phosphorylation. Intracellular replication of LF82 in the presence of PF-431396 was measured by total viable counts at (b) 6 h p.i., (c) 12 h p.i. and (d) 24 h p.i. PF-431396 hydrate was added to RAW 264.7 cells at concentrations of 0 µM (NC – negative control), 1 µM, 5 µM or 10 µM 1 h p.i. Statistical analyses were conducted using a one-way ANOVA. (ns, not significant, **P*<0.05, ***P*<0.01, ****P*<0.001, *****P*<0.0001). Data are representative of three independent biological experiments.

Intracellular survival of AIEC in macrophages

Given the previously reported role of Pyk2 in phagocytosis [28], we analysed the role of Pyk2 in phagocytosis of LF82 by RAW 264.7 cells. RAW 264.7 cells were infected with LF82 following a 1 h pre-treatment with PF-431396 hydrate before bacterial c.f.u. were counted. The highest concentration of inhibitor (10 µM) significantly impaired phagocytosis compared to cells that were untreated or treated with a lower concentration of inhibitor (Fig. 3a). Having established that PF-431396 hydrate blocks phagocytosis of LF82, further treatments to test any further inhibitory effects of this molecule were conducted post-phagocytosis of LF82. This was to ensure that any alteration in intracellular numbers of LF82 were not impacted by the inhibition of phagocytosis.

PF-431396 hydrate inhibition significantly reduces intra-macrophage LF82 burden

Intracellular replication is a hallmark of the AIEC phenotype. To determine the potential role of Pyk2 in intracellular replication of LF82, PF-431396 hydrate was added at concentrations of 0, 1, 5 or 10 μM at 1 h p.i. Intracellular bacteria numbers were measured using colony counts at 6, 12 and 24 h p.i. At 6 h p.i., there was no significant difference in intracellular bacterial numbers relative to the control at any concentration of PF-431396 hydrate (Fig. 3b). However, a significant reduction in intracellular LF82 numbers was seen at 12 h p.i. with 1 μM, 5 μM and 10 μM PF-431396 hydrate (Fig. 3c), and at 24 h p.i. for all concentrations of PF-431396 hydrate (Fig. 3d).

The interaction of intracellular pathogens with host cells is traditionally quantitated on a cellular population level. However, intracellular replication is heterogeneous, and infection of host cells with a clonal population of any intracellular pathogen frequently results in variable numbers of bacteria in individual host cells. To examine this, imaging flow cytometry was conducted to allow quantification of morphological cellular features and spatial distribution of fluorescent markers at the single-cell level in the heterogenous infected cell population. This made it possible to correlate acquired cellular images with specific cells, known as events, and accurately quantify intracellular bacteria.

To establish that transformation of LF82 with the fluorescent *rpsM*GFP reporter required for intracellular imaging did not alter the bacterial phenotype, growth rates of LF82 and LF82::*rpsM*GFP were assessed in the presence and absence of PF-431396 hydrate. There were no significant differences between any of the conditions assessed (Fig. S2a,b). An intracellular infection model, where the output is viable bacterial counts, was used to assess bacterial replication and survival in RAW 264.7 macrophages transformed with LF82::*rpsM*GFP at 6, 12 and 24 h (Fig. S2c–e). Comparison of intracellular replication of LF82 and LF82::*rpsM*GFP at 6, 12 and 24 h p.i. demonstrated that there was no significant difference in intracellular survival or replication between the strains (Fig. S2c–e), making LF82::*rpsM*GFP a suitable fluorescent reporter strain.

PF-431396 hydrate blocks intracellular LF82 replication without affecting overall numbers of infected cells

Given that LF82 infection of RAW 264.7 cells is heterogenous with potentially large numbers of intracellular bacteria, imaging flow cytometry was employed to quantitatively correlate the number of intracellular bacteria with the level of Pyk2 phosphorylation and activation in single cells. Single cells were gated as described in Fig. S3. Utilizing IDEAS imaging-flow analysis software (Luminex) spot count masks were created and used in conjunction with the erode mask to produce intracellular spot count profiles for each time point (Fig S4a–d).

To facilitate analysis cells were assigned to groups with those with greater than 10 bacteria deemed to have a 'high' bacterial burden, those with 6–10 bacteria assigned to an 'intermediate' bacterial burden, and those with five or less as having a 'low' bacterial burden. While assigning cells to these groups was arbitrary, cells were assigned to groups based on the hypothesis that cells with greater than 10 bacteria were more likely to be representative of those where intracellular replication of LF82 has taken place, whilst those with fewer than five bacteria were more likely to be indicative of bacterial phagocytosis rather than replication. Separating the infected macrophage population into distinct populations based on bacterial load is a significant step forward in understanding the dynamics of LF82 infection, which was previously determined using highly heterogenous populations of infected cells. For each of high, intermediate and low bacterial burdens the percentage of the total population was plotted at 6 h p.i. (Fig. 4a) and 12 h p.i. (Fig. 4b). Since treatment with PF-431396 hydrate was initiated post-phagocytosis, and therefore did not influence bacterial uptake by the macrophages, there were no significant differences observed in the ratio of infected:uninfected cells within any of the treatment groups. Untreated cells or those treated with 1 μM of PF-431396 hydrate had a significantly larger population of cells with high bacterial burden at both 6 h p.i. (18.57 and 16.96% of total cells, respectively) and 12 h p.i. (17.56 and 17.26%, respectively) compared to 10 μM treatment, which resulted in a significant decrease in the number of cells with a high bacterial burden (9.01% at 6 h p.i. and 6.87% at 12 h p.i., Fig. 4a, b). In cells treated with 10 μM PF-431396 hydrate, where less pPyk2 (Y402) protein was detectable, a significantly larger population of cells were observed to have a low bacterial burden at both 6 h p.i. (49.13%) and 12 h p.i. (53.43%), compared to untreated cells, which had 39.65% and 41.53% of cells deemed to have a low bacterial burden. This expansion of low bacterial burden cells in 10 μM PF-431396 hydrate treated cells was at the expense of those with a high bacterial burden, as there was a corresponding reduction in this subset. These data indicate that when the Pyk2/FAK axis is inhibited by PF-431396 hydrate it has a direct inhibitory effect on intracellular replication of LF82 in RAW 264.7 macrophages.

PF-431396 hydrate-mediated blocking of LF82 replication in macrophages significantly reduces TNFα secretion

High levels of TNFα are detected in CD patients and secretion of TNFα occurs post-infection of macrophages by AIEC [37]. High levels of TNFα are released as consequence of mucosal injury and transmural inflammation in CD, primarily from lamina propria mononuclear cells [38]. Additionally previous studies have highlighted a role for Pyk2 activation in TNFα secretion [39, 40]. Given intracellular numbers of LF82 were directly affected by addition of PF-431396 hydrate, we went on to determine if there was any downstream impact on TNFα release. Treatment of macrophages with 5 and 10 μM PF-431396 induced a significant

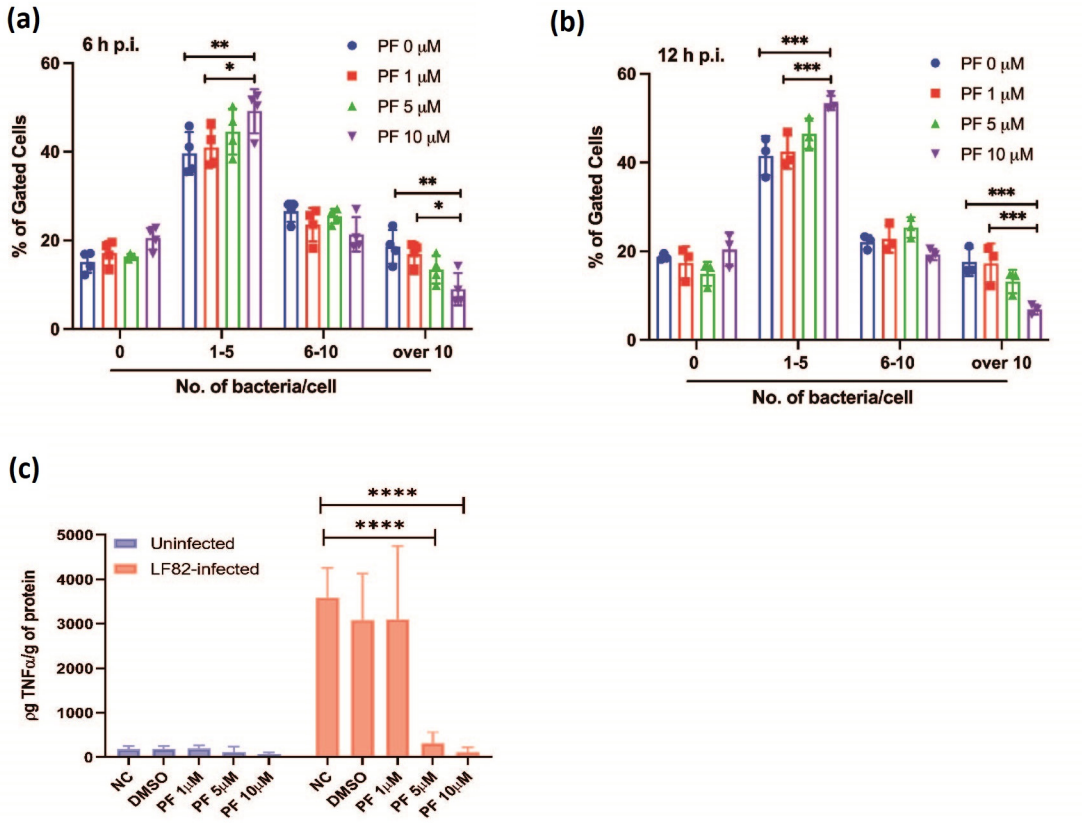

Fig. 4. Treatment with PF-431396 hydrate inhibits Pyk2 phosphorylation and reduces intra-macrophage LF82 burden and TNFα secretion. LF82::*rpsM*GFP burden in RAW 264.7 macrophages was analysed via imaging flow cytometry. The bacterial spot count profiles at 6 h p.i. (a) and 12 (b) h p.i. were separated into: groups representing uninfected cells (0 bacterium); cells with a low infection count (1–5 bacteria per cell); medium infection count (6–10 bacteria per cell); and highly infected cells (>10 bacteria per cell) where PF refers to concentration of PF-431396 hydrate added. Statistical analysis was conducted using a two-way ANOVA test. (ns, not significant, **P*<0.05, ***P*<0.01, ****P*<0.001, *****P*<0.0001). Data are representative of three independent biological replicates. (c) Comparison of TNF-α section levels from supernatants of infected or uninfected RAW 264.7 cells. RAW 264.7 cells were activated by LPS overnight then infected or uninfected with LF82 for 1 h followed by treatment with PF-431396 hydrate for 6 h. At 6 h p.i., TNFα levels in supernatants were examined by ELISA. Values are mean±SD (*n*=3 per group). Statistical analysis was conducted using a two-way ANOVA test (ns, not significant, **P*<0.05, ***P*<0.01, ****P*<0.001, *****P*<0.0001).

reduction in TNFα release (between 15- and 40-fold) (Fig. 4c). This reduction was not seen in untreated macrophages or those treated with 1 μM inhibitor (Fig. 4c). These decreases in TNFα release could not be attributed to increased toxicity due to the inhibitor (Fig. S1). While it is difficult to conclusively conclude that this reduction in TNFα secretion is a direct result of kinase inhibition, rather than an indirect effect of the lower intracellular burden of LF82, the significant decrease in TNFα release that was observed at 5 μM PF-431396 hydrate was not associated with a reduction in intracellular burden (Fig. 4a, b). After establishing that PF-431396 hydrate reduced intra-macrophage replication of LF82, and secretion of TNFα by LF82 infected macrophages, we examined the role of PF-431396 hydrate more widely. Similar effects of PF-431396 hydrate inhibition were also observed in macrophages infected with *Salmonella enterica* serovar Typhimurium (*S.* Typhimurium) strain SL1344 and clinical isolates of *E. coli* from CD patients, although the observed drop in c.f.u. was only significant with SL1344 infection and clinical isolates B115 and B125 at 24 h p.i. (Fig. 5a, b). PF-431396 hydrate significantly decreased TNFα secretion in macrophages, which had taken up clinical isolates of *E. coli* from CD patients, with this effect observed across all isolates at 24 h p.i. There were similar significant reductions in TNFα secretion in uninfected cells and those exposed to both commensal *E. coli* and *S.* Typhimurium (Fig. 5c, d).

DISCUSSION

Proline tyrosine kinase 2 (Pyk2) has been identified as a susceptibility locus for IBD risk [18]. However, an association between Pyk2 and AIEC, the *E. coli* pathotype consistently overrepresented in the CD intestinal microbiome, has never been investigated. For the first time, our work has demonstrated a direct link between AIEC intracellular replication and activation of Pyk2. Here we

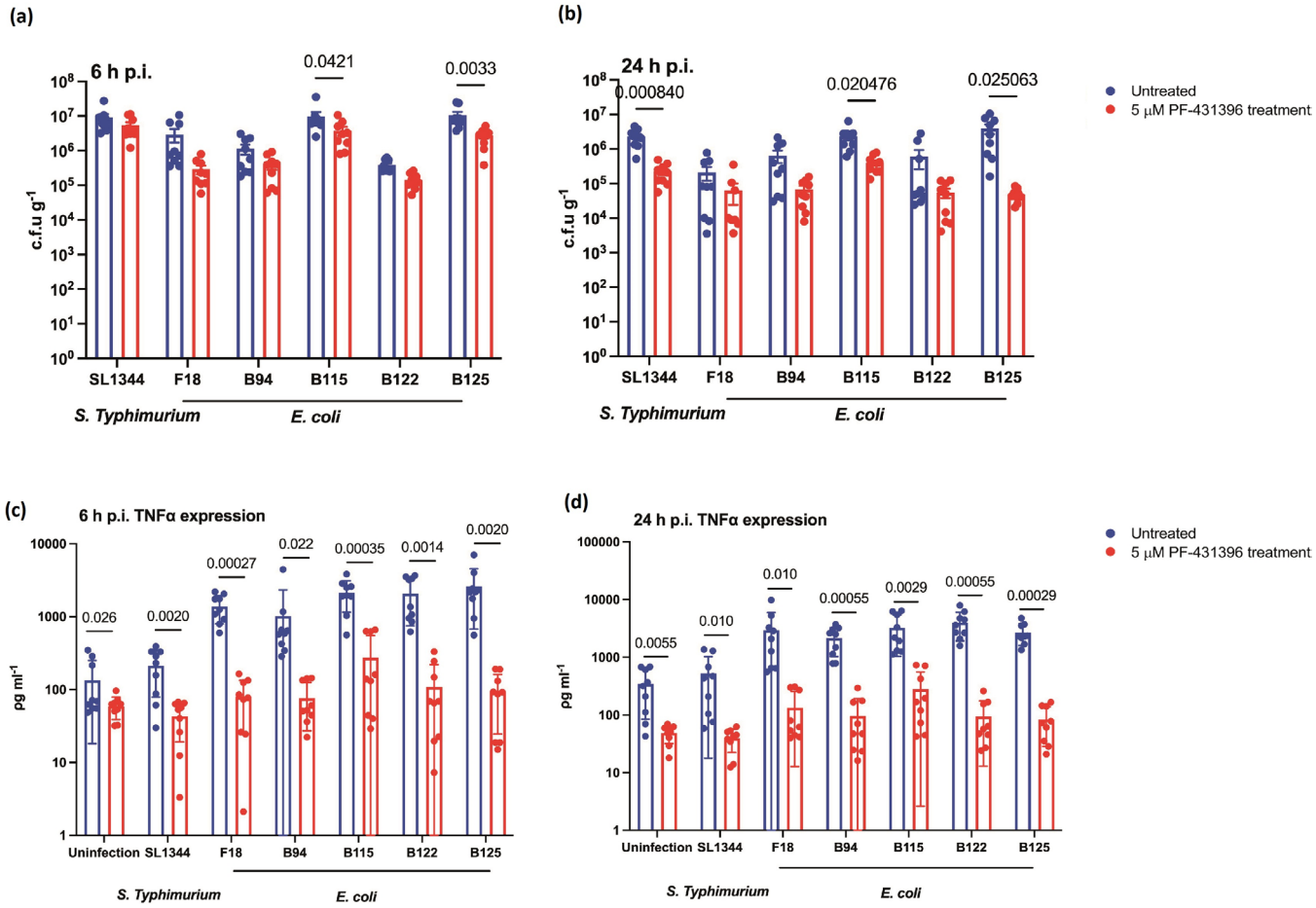

Fig. 5. Pyk2 inhibition reduces AIEC clinical isolate intramacrophage burden and TNFα release. RAW 264.7 macrophages were infected with AIEC type strain, LF82, commensal strain *E. coli* F18, *Salmonella* Typhimurium strain SL1344 and AIEC clinical isolates B94, B115, B122, and B125 for 1 h with m.o.i. of 100, followed by treatment with or without 5 μM PF-431396 hydrate for a further 6, or 24 h p.i. (a, b) intracellular bacterial numbers were determined by c.f.u. counts. (c, d) ELISAs were conducted to detect the secretion of TNFα from uninfected or infected macrophages with or without 5 μM PF-431396 hydrate treatment. Data displayed are of three independent experimental replicates, with each experiment including three independent biological replicates. Data are expressed as mean±SD; data were analysed using unpaired multiple *t*-tests.

show that Pyk2 plays a dual role in AIEC infection, by initially impacting bacterial phagocytosis before subsequently facilitating AIEC replication and survival within macrophages.

To date, only infection by *Y. pseudotuberculosis* has been shown to require Pyk2 for bacterial phagocytosis by macrophages [24, 41]. Previous studies identified that the *Yersinia* outer surface protein, invasin, provides high-affinity interactions with host cell surface β1 integrin receptors [42]. Binding of integrins then induces integrin clustering and sustained activation of Pyk2, which has been implicated in numerous actin-based cellular processes including cell cycle progression, adhesion and migration [43]. Consistent with this, Bruce-Staskal *et al.* [44] have shown that *Yersinia* uptake involved a complex interplay in Cas, FAK, Pyk2 and Rac1 cell signalling [44]. Through inhibition of Pyk2 phosphorylation through the FAK/Pyk2 inhibitor PF-431396 hydrate, we first demonstrated that AIEC phagocytosis (Fig. 3) was impeded, again reflecting the known role of phosphorylation of Pyk2, and the possible involvement of FAK alongside, in the regulation of phagocytosis [28, 31]. We then determined that in addition, the AIEC type strain LF82 is reduced intracellularly in a dose-dependent manner in response to inhibition by PF-431396 hydrate.

Phagocytosis is initiated by macrophage cell-membrane Toll-like receptor (TLR) 4 and TLR 5, which recognize bacterial extracellular structures such as fimbriae, flagella, LPS and peptidoglycan [45]. Upon phagocytosis of microbial pathogens, TLR4 recruits MyD88 initiating the nuclear factor-κB (NF-κB) signalling cascade [46]. Xi *et al.* [47] showed that Pyk2 interacts with MyD88 and regulates MyD88-mediated NF-κß activation in macrophages with resulting TNFα secretion [47]. Secretion of high levels of TNFα are associated with AIEC replication and survival within macrophages without inducing cell death [37]. To date, the most effective CD treatments include anti-TNFα or anti-integrin treatments to reduce the circulating concentration of TNFα [48]. However, the cellular mechanisms underpinning the effect of TNFα on AIEC replication have remained elusive. *In vivo*

infection experiments have demonstrated that CD mucosa-associated *E. coli* killing by macrophages could be inhibited by microbial mannan in a TLR4 and MyD88-dependent manner [49]. Taken together, this suggests a mechanism supporting AIEC replication and survival within macrophages via a TLR4-MyD88-Pyk2-NF-κß-TNFα cascade.

Intracellular bacterial replication within macrophages is a characteristic trait of AIEC infection. To investigate this, we analysed intracellular replication using colony counts and imaging flow cytometry. Both methods indicated that PF-431396 hydrate-mediated inhibition significantly decreases intracellular replication of AIEC at 12 h p.i. compared to untreated cells. While no significant differences in intracellular bacteria were observed using viable counts after 6 h (Fig. 2a), there was a significant change in intracellular bacterial numbers observed using imaging flow cytometry. While this tandem approach gives a greater overall picture of the role of Pyk2 in AIEC infection, the contrasting outputs from each at 6 h p.i. are noteworthy. Viable counts are most commonly used in infection studies, but they are limited by the need for sample processing and subsequent growth of bacteria before counting. They are also heavily dependent on the successful removal of extracellular bacteria by antibiotics. In such a heterogenous mixture of infected cells, the viable count approach merely provides a broad overview of a population that is intrinsically different, and in all likelihood, it will be releasing diverse levels of cytokines and undergoing cell death at different rates at any given moment. In addition, within any well where bacteria are added the large proportion of cells within that well that remain uninfected likely mask the phenotype of infected cells within the same well. So the phenotype presented from such a well represents a mix of both uninfected and infected cells, rather than just infected cells, which was the target of the study. In contrast, imaging flow cytometry here allowed the determination of bacterial number at the single-cell level and permitted the correlation of bacterial load and Pyk2 status within each individual cell. It also allowed accurate determination of intracellular numbers of persistent, viable, non-culturable cells, which would be excluded using the viable count method. In addition, extracellular or attached bacteria could be discounted and uninfected macrophages within a well of infected cells could also be identified and analysed as a separate subpopulation. The high-throughput nature of imaging flow cytometry provided sufficient data to enable trends to be determined within infected cells, such as Pyk2 status versus intracellular bacterial load. However, as with any approach there are limitations. Some bacteria may be lysed or non-viable, but their fluorescent signal may still be temporarily detectable. Additionally, the masks applied during analysis to determine cell size will never be 100% accurate for the entire population of cells, and there will always be cells that do not conform to the parameters set. However, applying this approach to phenotypically characterize a heterogenous population of infected cells based on their intracellular bacterial load is a significant step forward in studying infection at the level of the cell rather than the level of the well.

To date, AIEC infection has been poorly understood relative to other pathogens, it's paucity of virulence factors rendering it difficult to study via traditional microbiological approaches of mutation and testing. Its virulence has been attributed to its unique ability to survive and rapidly replicate within macrophages, while inducing a strong inflammatory response in the form of TNFα release. Here we focused on the AIEC–host interaction through high-throughput imaging and phenotyping of infected cell populations and studying them in the context of Pyk2, a known effector of gut inflammation in the intestine in the context of IBD [20, 29, 30]. Our approach enabled the removal of phenotypic noise introduced by the presence of many uninfected cells within infected-cell populations, giving a clearer picture of the AIEC–macrophage relationship. Our results identified a role for Pyk2 in facilitating AIEC uptake by macrophages, as previously reported for other pathogens, but remarkably also showed for the first time another role for Pyk2 in facilitating AIEC intra-macrophage replication and TNFα release. While the focus of this study was Pyk2 the inhibitor used here, PF-431396 hydrate, also inhibits another kinase, FAK so a role for it in these interactions cannot be discounted. However, pharmaceutical intervention to block the function of these kinases successfully blocked AIEC intracellular replication and subsequent TNFα release, identifying a potential pathway towards an intervention strategy for CD patients where AIEC are dominant in the intestinal microbiome. The importance of these findings was underlined with reproduction of these phenotypes with clinical isolates of AIEC, while the relevance for other enteric pathogens was also shown through PF-431396 hydrate inhibition also significantly altering the course of *Salmonella* Typhimurium infection.

Given the short-term nature of the experiments here, with infection proceeding for less than 48 h, the similarity in outcomes between *S*. Typhimurium and AIEC during this acute period of infection is not unexpected. However, in the context of AIEC, and its exacerbation of gut inflammation in CD, the repercussions of the findings are more wide ranging. An ability to block replication and TNFα release in persistent infection would offer clear therapeutic benefits, and alongside other studies implicating Pyk2 in IBD may point towards it being an outstanding target in IBD. The similarity in infection strategy between *S*. Typhimurium as an acute pathogen in terms of its survival in macrophages, and AIEC, which persists intracellularly, points to the inhibition employed here being more applicable across a range of intracellular pathogens. Indeed, recent work has highlighted a role for Pyk2 and FAK in viral infection where their inhibition promotes mouse survival post-sepsis [50, 51]. Together these findings point towards the Pyk2/FAK axis as being critical in both infection and inflammation control.

Funding information
The author(s) received no specific grant from any funding agency.

Acknowledgements
The authors would like to thank Dr Leandro Lemgruber Soares and Susan Gannon at Glasgow Image Facility for helpful experimental advice. This work was funded by Biotechnology and Biological Sciences Research Council grants BB/K008005/1 and BB/P003281/1 to D.M.W. and through a PhD studentship to G.F. from the College of Science and Health Professions, King Saud bin Abdulaziz University for Health Sciences, Jeddah, Saudi Arabia.

Conflicts of interest
The authors declare that there are no conflicts of interest.

Reference

1. Heresbach D, Alexandre JL, Branger B, Bretagne JF, Cruchant E, *et al*. Frequency and significance of granulomas in a cohort of incident cases of Crohn's disease. *Gut* 2005;54:215–222.
2. Molnár T, Tiszlavicz L, Gyulai C, Nagy F, Lonovics J. Clinical significance of granuloma in Crohn's disease. *World J Gastroenterol* 2005;11:3118–3121.
3. Shen Z, Zhu C, Quan Y, Yuan W, Wu S, *et al*. Update on intestinal microbiota in Crohn's disease 2017: mechanisms, clinical application, adverse reactions, and outlook. *J Gastroenterol Hepatol* 2017;32:1804–1812.
4. Miquel S, Peyretaillade E, Claret L, de Vallée A, Dossat C, *et al*. Complete genome sequence of Crohn's disease-associated adherent-invasive *E. coli* strain LF82. *PLoS One* 2010;5:e12714.
5. Barnich N, Darfeuille-Michaud A. Adherent-invasive *Escherichia coli* and Crohn's disease. *Curr Opin Gastroenterol* 2007;23:16–20.
6. Darfeuille-Michaud A, Boudeau J, Bulois P, Neut C, Glasser AL, *et al*. High prevalence of adherent-invasive *Escherichia coli* associated with ileal mucosa in Crohn's disease. *Gastroenterology* 2004;127:412–421.
7. Glasser A-L, Boudeau J, Barnich N, Perruchot M-H, *et al*. Adherent invasive *Escherichia coli* strains from patients with Crohn's disease survive and replicate within macrophages without inducing host cell death. *Infect Immun* 2001;69:5529–5537.
8. Bringer M-A, Glasser A-L, Tung C-H, Meresse S, Darfeuille-Michaud A. The Crohn's disease-associated adherent-invasive *Escherichia coli* strain LF82 replicates in mature phagolysosomes within J774 macrophages. *Cell Microbiol* 2006;8:471–484.
9. Becker T, Volchuk A, Rothman JE. Differential use of endoplasmic reticulum membrane for phagocytosis in J774 macrophages. *Proc Natl Acad Sci*2005;102:4022–4026.
10. Desjardins M. Biogenesis of phagolysosomes: the "kiss and run" hypothesis. *Trends Cell Biol* 1995;5:183–186.
11. Yang Y, Liao Y, Ma Y, Gong W, Zhu G. The role of major virulence factors of AIEC involved in inflammatory bowl disease—a mini-review. *Appl Microbiol Biotechnol* 2017;101:7781–7787.
12. Ohno H. Intestinal M cells. *J Biochem* 2016;159:151–160.
13. Bain CC, Mowat AM. Macrophages in intestinal homeostasis and inflammation. *Immunol Rev* 2014;260:102–117.
14. Schmitz H, Fromm M, Bentzel CJ, Scholz P, Detjen K, *et al*. Tumor necrosis factor-alpha (TNFalpha) regulates the epithelial barrier in the human intestinal cell line HT-29/B6. *J Cell Sci* 1999;112:137–146.
15. Lissner D, Schumann M, Batra A, Kredel LI, Kühl AA, *et al*. Monocyte and M1 macrophage-induced barrier defect contributes to chronic intestinal inflammation in IBD. *Inflamm Bowel Dis* 2015;21:1297–1305.
16. Hanauer SB, Feagan BG, Lichtenstein GR, Mayer LF, Schreiber S, *et al*. Maintenance infliximab in Crohn's disease: the ACCENT I randomised trial. *Lancet* 2002;359:1541–1549.
17. Rutgeerts P, Van Assche G, Sandborn WJ, Wolf DC, Geboes K, *et al*. Adalimumab induces and maintains mucosal healing in patients with Crohn's disease: data from the EXTEND trial. *Gastroenterology* 2012;142:1102–1111.
18. Liu JZ, van Sommeren S, Huang H, Ng SC, Alberts R, *et al*. Association analyses identify 38 susceptibility loci for inflammatory bowel disease and highlight shared genetic risk across populations. *Nat Genet* 2015;47:979–986.
19. Williams LM, Ridley AJ. Lipopolysaccharide induces actin reorganization and tyrosine phosphorylation of Pyk2 and paxillin in monocytes and macrophages. *J Immunol* 2000;164:2028–2036.
20. Ryzhakov G, Almuttaqi H, Corbin AL, Berthold DL, Khoyratty T, *et al*. Defactinib inhibits PYK2 phosphorylation of IRF5 and reduces intestinal inflammation. *Nat Commun* 2021;12:6702.
21. Kohno T, Matsuda E, Sasaki H, Sasaki T. Protein-tyrosine kinase CAKbeta/PYK2 is activated by binding Ca2+/calmodulin to FERM F2 alpha2 helix and thus forming its dimer. *Biochem J* 2008;410:513–523.
22. Zhu X, Bao Y, Guo Y, Yang W. Proline-rich protein tyrosine kinase 2 in inflammation and cancer. *Cancer* 2018;10:139.
23. Zhao M, Finlay D, Zharkikh I, Vuori K, Buday L. Novel role of Src in priming Pyk2 phosphorylation. *PLoS One* 2016;11:e0149231.
24. Hudson KJ, Bliska JB, Bouton AH. Distinct mechanisms of integrin binding by *Yersinia pseudotuberculosis* adhesins determine the phagocytic response of host macrophages. *Cell Microbiol* 2005;7:1474–1489.
25. Schaller MD. Cellular functions of FAK kinases: insight into molecular mechanisms and novel functions. *J Cell Sci* 2010;123:1007–1013.
26. Liu S, Chen L, Xu Y. Significance of PYK2 level as a prognosis predictor in patients with colon adenocarcinoma after surgical resection. *Onco Targets Ther* 2018;11:7625–7634.
27. Okigaki M, Davis C, Falasca M, Harroch S, Felsenfeld DP, *et al*. Pyk2 regulates multiple signaling events crucial for macrophage morphology and migration. *Proc Natl Acad Sci*2003;100:10740–10745.
28. Paone C, Rodrigues N, Ittner E, Santos C, Buntru A, *et al*. The tyrosine kinase Pyk2 contributes to complement-mediated phagocytosis in murine macrophages. *J Innate Immun* 2016;8:437–451.
29. Thomas KS, Owen KA, Conger K, Llewellyn RA, Bouton AH, *et al*. Non-redundant functions of FAK and Pyk2 in intestinal epithelial repair. *Sci Rep* 2019;9:4497.
30. Canino J, Guidetti GF, Galgano L, Vismara M, Minetti G, *et al*. The proline-rich tyrosine kinase Pyk2 modulates integrin-mediated neutrophil adhesion and reactive oxygen species generation. *Biochim Biophys Acta Mol Cell Res* 2020;1867:118799.
31. Naser R, Aldehaiman A, Díaz-Galicia E, Arold ST. Endogenous control mechanisms of FAK and PYK2 and their relevance to cancer development. *Cancers (Basel)* 2018;10:196.
32. Darfeuille-Michaud A, Neut C, Barnich N, Lederman E, Di Martino P, *et al*. Presence of adherent *Escherichia coli* strains in ileal mucosa of patients with Crohn's disease. *Gastroenterology* 1998;115:1405–1413.
33. Roe AJ, Yull H, Naylor SW, Woodward MJ, Smith DGE, *et al*. Heterogeneous surface expression of EspA translocon filaments by. *Society* 2003;71:5900–5909.
34. Buckbinder L, Crawford DT, Qi H, Ke HZ, Olson LM, *et al*. Proline-rich tyrosine kinase 2 regulates osteoprogenitor cells and bone formation, and offers an anabolic treatment approach for osteoporosis. *Proc Natl Acad Sci U S A* 2007;104:10619–10624.
35. Mills RD, Mita M, Nakagawa J, Shoji M, Sutherland C, *et al*. A role for the tyrosine kinase Pyk2 in depolarization-induced contraction of vascular smooth muscle. *J Biol Chem* 2015;290:8677–8692.
36. Schneider CA, Rasband WS, Eliceiri KW. NIH image to imageJ: 25 years of image analysis. *Nat Methods* 2012;9:671–675.
37. Bringer MA, Billard E, Glasser AL, Colombel JF, Darfeuille-Michaud A. Replication of Crohn's disease-associated AIEC within macrophages is dependent on TNF-α secretion. *Lab Invest* 2012;92:411–419.

38. Adegbola SO, Sahnan K, Warusavitarne J, Hart A, Tozer P. Anti-TNF therapy in Crohn's Disease. *Int J Mol Sci* 2018;19:1–21.
39. Murphy JM, Jeong K, Rodriguez YAR, Kim JH, Ahn EYE, *et al*. FAK and Pyk2 activity promote TNF-α and IL-1β-mediated pro-inflammatory gene expression and vascular inflammation. *Sci Rep* 2019;9:7617.
40. Yang C-M, Lee I-T, Hsu R-C, Chi P-L, Hsiao L-D. NADPH oxidase/ROS-dependent PYK2 activation is involved in TNF-α-induced matrix metalloproteinase-9 expression in rat heart-derived H9c2 cells. *Toxicol Appl Pharmacol* 2013;272:431–442.
41. Owen KA, Thomas KS, Bouton AH. The differential expression of *Yersinia pseudotuberculosis* adhesins determines the requirement for FAK and/or Pyk2 during bacterial phagocytosis by macrophages. *Cell Microbiol* 2007;9:596–609.
42. Wiedemann A, Linder S, Grassl G, Albert M, Autenrieth I, *et al*. *Yersinia enterocolitica* invasin triggers phagocytosis via beta1 integrins, CDC42Hs and WASp in macrophages. *Cell Microbiol* 2001;3:693–702.
43. Avraham H, Park SY, Schinkmann K, Avraham S. RAFTK/Pyk2-mediated cellular signalling. *Cell Signal* 2000;12:123–133.
44. Bruce-Staskal PJ, Weidow CL, Gibson JJ, Bouton AH. Cas, Fak and Pyk2 function in diverse signaling cascades to promote *Yersinia* uptake. *J Cell Sci* 2002;115:2689–2700.
45. Smith EJ, Thompson AP, Clarke DJ. Pathogenesis of adherent–invasive. 2013;8:1289–1300.
46. Sanjuan MA, Milasta S, Green DR. Toll-like receptor signaling in the lysosomal pathways. *Immunol Rev* 2009;227:203–220.
47. Xi C-X, Xiong F, Zhou Z, Mei L, Xiong W-C. PYK2 interacts with MyD88 and regulates MyD88-mediated NF-kappaB activation in macrophages. *J Leukoc Biol* 2010;87:415–423.
48. Larabi A, Barnich N, Nguyen HTT. New insights into the interplay between autophagy, gut microbiota and inflammatory responses in IBD. *Autophagy* 2020;16:38–51.
49. Mpofu CM, Campbell BJ, Subramanian S, Marshall-Clarke S, Hart CA, *et al*. Microbial mannan inhibits bacterial killing by macrophages: a possible pathogenic mechanism for Crohn's disease. *Gastroenterology* 2007;133:1487–1498.
50. Rodrigues V, Taheraly S, Maurin M, San-Roman M, Granier E, *et al*. Release of HIV-1 particles from macrophages is promoted by an anchored cytoskeleton and driven by mechanical constraints. *J Cell Sci* 2022;135:jcs260511.
51. Alves GF, Aimaretti E, Einaudi G, Mastrocola R, de Oliveira JG, *et al*. Pharmacological inhibition of FAK-Pyk2 pathway protects against organ damage and prolongs the survival of septic mice. *Front Immunol* 2022;13:837180.

Edited by: S. P Diggle and D. J. Clarke